Renal denervation improves renal remodelling and function in a model for hypertension and metabolic syndrome---role of RAGE/sRAGE balance

Simina-Ramona Selejan 1*, Dominik Linz 1*, Matthias Hohl 1, Anna-Maria Tatu 1, Philipp Markwirth 1, Timotheus Speer 2, Joachim Jankowski 3,4, Andrey Kazakov 1, Christian Werner 1, Felix Mahfoud 1, Michael Böhm 1

*Selejan S and Linz D contributed equally to this study

1 Department of Internal Medicine III, Cardiology, Angiology and Intensive Care Medicine,

Saarland University, Homburg/Saar, Germany

2 Department of Internal Medicine IV (Nephrology and Hypertension),

Saarland University, Homburg/Saar, Germany

3 Institute for Molecular Cardiovascular Research, RWTH Aachen University Hospital, Aachen, Germany.

4 School for Cardiovascular Diseases, Maastricht University, Maastricht, The Netherlands

Correspondence to:

Simina-Ramona Selejan, MD

Department of Internal Medicine III

Kirrbergerstr. 100, Geb. 41.1 (IMED)

University and University Hospital of Saarland

D-66421 Homburg/Saar; Germany

Phone : +49-6841-16-15031

Fax : +49-6841-16-15032

e-mail: simina.selejan@uks.eu

Abstract

Renal denervation (RDN) reduces renal sympathetic activity and blood pressure, but potential renal protective effects are not well studied. The multi-ligand receptor "Receptor for Advanced Glycation End-products" (RAGE) activates mechanisms involved in inflammation-associated tissue remodelling. Circulating soluble RAGE (sRAGE), comprising only the RAGE extracellular ligand binding domain, serves as anti-inflammatory decoy receptor. We investigated RAGE/sRAGE and RAGE-ligand expression (Carboxymethyllysine (CML) and High-mobility-group-box-1 protein (HMGB1)) in kidney remodelling and function by modulation of sympathetic nervous system with renal denervation (RDN) in a rat model of hypertension with metabolic syndrome and coexistent renal dysfunction (Spontaneously Hypertensive Obese Rat (SHRob)) compared with arterial hypertension alone in Spontaneously Hypertensive Rats (SHR) and with non-hypertensive, non-obese (control) rats. RDN in SHRob (SHRobRDN) reduced mean systolic blood pressure by -45 mmHg compared to SHRob ($p=0.008$). This was accompanied by a reduction in kidney fibrosis (-43%, $p=0.03$) and improved glomerular score (-21%, $p<0.001$) resulting in improved kidney function (+130% GFR, $p<0.001$; -35% creatinine, $p=0.04$; -54% albuminuria, $p<0.001$) in SHRobRDN compared with SHRob. In SHRob, renal RAGE was increased (+2500%, $p=0.002$) and sRAGE was decreased (-59%, $p=0.04$) compared with controls. RDN reduced RAGE protein expression (-59% versus SHRob, $p=0.03$) and significantly increased sRAGE levels (+131% versus SHRob, $p=0.04$). Furthermore, RDN induced a significant decrease in kidney RAGE-ligand levels in SHRob (-73% CML, $p=0.003$, and -88% HMGB1, $p=0.01$, compared with SHRob).

Our findings support the concept that suppression of renal sympathetic nerve activity by RDN may prevent kidney damage in metabolic syndrome by modulating RAGE/sRAGE balance.

Translational statement

Renal denervation reduces renal norepinephrine spill over and has been shown to reduce blood pressure in clinical trials. Renal RAGE/sRAGE dysbalance leads to kidney injury in several pathophysiologic conditions. Our study shows that renal denervation improves RAGE/sRAGE balance, renal interstitial remodelling and renal function in rats with metabolic syndrome, hypertension and chronic kidney disease. The results presented herein provide the physiological basis for clinical studies in these conditions. Randomized sham-controlled trials are needed to assess potential nephro-protective effects of RDN in metabolic syndrome with arterial hypertension and chronic kidney disease.

Introduction

Renal denervation (RDN) reduces renal norepinephrine spill over but also systemic sympathetic activation and is currently under investigation for uncontrolled arterial hypertension (**1-4**). In previous studies, we provided evidence that RDN prevented left ventricular interstitial remodelling in a rat model with metabolic syndrome, hypertension and coexistent renal dysfunction (Spontaneously Hypertensive Obese rats (SHRob) (**5-6**) consistent with ventricular (**7-8**) and atrial (**9**) de-remodelling after RDN in hypertensive patients. Mechanistically, we showed an influence of the sympathetic autonomic nervous system on the "RAGE/sRAGE system" (**5**). RAGE (Receptor for Advanced Glycation End-products) is a pro-inflammatory and pro-fibrotic, multi-ligand membrane-bound receptor (**10**), which is shedded to its soluble form, called sRAGE, by metalloprotease-mediated cleavage (**11-12**). sRAGE exerts anti-inflammatory effects by competing with RAGE for ligand binding and also blocking RAGE itself (**10, 13**). The representative advanced glycation end-product carboxymethyllysine (CML) and High-mobility-group-box-1 protein (HMGB1) are two important pro-fibrotic and pro-inflammatory RAGE-ligands involved in RAGE-mediated organ remodelling (**5, 10**). Whether improvement in renal RAGE/sRAGE balance, kidney function and remodelling processes occur upon RDN, is unknown. This study aimed to characterize the influence of the sympatho-adrenergic system and its modulation by RDN on renal interstitial remodelling, function and regulation of the RAGE/sRAGE-system and its ligands CML and HMGB1 in metabolic syndrome with renal dysfunction.

Results

Metabolic and hemodynamic parameters

Metabolic and hemodynamic characterizations of both SHRob and SHR models have recently been published (**6, 14**). The main metabolic and renal parameters are summarized in **Table 1**. In brief, SHR and SHRob both showed increased systolic blood pressure as determined by telemetry in awake rats (RR systolic 199±5.6 mmHg in SHR, 224±5 mmHg in SHRob, versus 116±2.9 mmHg in controls, $p<0.001$). Blood pressure was reduced by RDN (179±12 mmHg in SHRobRDN, $p=0.008$ versus SHRob). SHRob displayed a reduction in kidney function with decreased glomerular filtration rate (GFR 0.18 l/kg/h in SHRob versus 0.41 l/kg/h in SHR and 0.61 l/kg/h in controls, $p<0.001$) and increased creatinine concentrations (29±0.6 umol/l in SHRob, 25±2.3 umol/l in SHR and 16.3±2.1 umol/l in Controls, $p=0.01$ SHRob versus controls). Fasting insulin levels were increased in SHRob, however fasting glucose and HbA1C values remained within the normal range (**Table 1**). Cholesterol and triglyceride concentrations were significantly increased in SHRob as compared with normotensive, non-obese controls and SHR (**Table 1**). RDN improved parameters of renal function such as GFR, and albuminuria (**Table 1**). However, RDN induced a numerical, albeit insignificant decrease in hyperinsulinemia and had no effect on hyperlipidemia or body weight (**Table 1**). Renal norepinephrine levels were significantly decreased after RDN, indicating effective neural denervation (103±5.5 pg/ml in SHRob versus 8.2±2.2 pg/ml in SHRobRDN, $p<0.001$).

Renal structural and interstitial remodelling

Histological analysis of the kidney (Picro-Sirius Red staining) (**Table 1, Figure 1A-B**) demonstrated an increase in tubulointerstitial collagen deposition in SHRob (7.2±1.2%) as compared with SHR (2.9±0.3%) and normotensive controls (2.4±0.3%, p<0.01 for each comparison), which was significantly reduced by RDN (4.1±0.4% in SHRobRDN vs. 7.2±1.2% in SHRob, p=0.03). In SHRob rats, a shift in the ratio of collagen type I (red-yellow fibers) to collagen type III (green fibers) as assessed by polarization microscopy (**Figure 1C-D)** was observed. Semiquantitative scoring of glomerular sclerosis (hematoxylin/eosin (H.E.) staining; **Table 1, Figure 1E-F**) revealed increased glomerular injury in SHRob (2.3±0.07) as compared with SHR (0.9±0.05) and controls (0.7±0.08, p<0.001 for each comparison) with tubular protein casts as a sign of increased glomerular damage and permeability. Treatment with RDN attenuated glomerular injury as shown by a reduction in glomerular score (1.8±0.09 in SHRobRDN, p<0.001 versus SHRob).

Renal RAGE/sRAGE

Renal RAGE protein as assessed by fluorescence microscopy (**Figure 2A**) and by Western blot analysis (**Table 1, Figure 2B-C**) was markedly increased in SHRob as compared with SHR as well as with normotensive controls (10.6±2.2 AU/GAPDH in SHRob versus 2.9±0.8 AU/GAPDH in SHR and 0.4±0.1 AU/GAPDH in controls; p<0.003 for each comparison). Kidney sRAGE levels (**Table 1, Figure 2D**) were significantly decreased in SHRob compared with lean, non-hypertensive controls (3.6±0.1 AU/GAPDH in SHRob versus 11.9±3.3 in controls, p=0.04) but were significantly restored after RDN (11.3±1.9 AU/GAPDH in SHRobRDN, p=0.04 versus SHRob). Renal RAGE expression showed a positive correlation with kidney norepinephrine concentration **(Figure 2 E-F**; r=0.75, p=0.007, n=10 SHRob+SHRobRDN), while renal sRAGE correlated negatively (r= -0.8; p=0.02, n=10).

RDN decreases RAGE-ligands Carboxymethyllysine (CML) and High-mobility-group-box-1 protein (HMGB1) in kidney tissue

Renal levels of the AGE CML (**Table 1, Figure 3A**) proved to be increased in SHR (6.8±1.5 AU/GAPDH) and SHRob (8.3±0.9 AU/GAPDH) compared with controls (1.98±0.5 AU/GAPDH, p=0.003-0.02 for each comparison). RDN resulted in a significant reduction of kidney CML content (**Figure 3A**; 2.2±0.4 AU/GAPDH in SHRobRDN versus 8.3±0.9 AU/GAPDH in SHRob, p=0.003) reaching levels of normotensive controls (1.98±0.5 AU/GAPDH in controls). Kidney HMGB1 levels were significantly higher in SHRob when compared with SHR and normotensive controls (**Table 1; Figure 3B**; 15.9±6.2 AU/GAPDH in SHRob versus 1.78±0.5 AU/GAPDH in SHR and 1.1±0.2 AU/GAPDH in controls; p<0.01 for each comparison). RDN significantly reduced renal HMGB1 (**Figure 3B**; 1.98±0.7 AU/GAPDH in SHRobRDN versus 15.9±6.2 AU/GAPDH in SHRob, p=0.01).

ß-adrenergic stimulation of renal fibroblasts and human embryonic kidney (HEK) cells increases RAGE expression and decreases sRAGE secretion

Renal fibroblasts and HEK cells were repeatedly stimulated (every 24 hours for 72 hours) with the ß1+ß2-adrenoreceptor agonist isoproterenol (0.1 µmol/l), which led to a significant increase in RAGE content in the cell membrane (+430% increase in HEK (**Figure 4A**), +35% in renal fibroblasts (**Figure 5A**)). Simultaneously, sRAGE shedding into the supernatant was reduced by isoproterenol treatment (after 72h -46% reduction in HEK (**Figure 4B**), and -65% reduction in renal fibroblasts (**Figure 5B**)). To identify the ß-adrenergic receptor subtype involved, we co-stimulated with ß-adrenergic receptor antagonists with ß1- or ß2 subtype selectivity (CGP 201712A (ß1-selective) or ICI 118.551 (ß2-selective)) simultaneously to isoproterenol. The isoproterenol-induced RAGE expression (Figures 4A-5A) was reversed by the ß1-adrenergic receptor blockade with CGP, while sRAGE shedding recovered with ß2-adrenergic receptor blockade by ICI (**Figures 4B-5B**). We observed differently pronounced but similar effects in both cell types.

Discussion

The model of SHRob comprises three concomitant risk factors: arterial hypertension (**1**), obesity and hyperinsulinemia (**15-19**), all of which are well known to cause renal damage. These conditions are associated with a RAGE/sRAGE imbalance (**20-21**) and accumulation of AGEs contributing to maladaptive remodelling processes in the kidney (**15-19**). RDN has been shown to reduce blood pressure in several randomized, sham-controlled trials and stabilized renal function (**22-23**).

Increased glomerular sclerosis and interstitial fibrosis developed in the kidneys of SHRob, though significant reduction in fibrosis was documented in the RDN group. RAGE is known to increase collagen type I transcription (**24**). Considering the polarized microscopy analysis, the main part of the observed renal fibrosis appears to be caused by an increase in type I collagen with augmented collagen type I/collagen type III ratio. Therefore, this fibrosis pattern is in agreement with a RAGE-mediated mechanism. This collagen-shift has been well studied in the heart in the context of ventricular stiffness (**25**).

In the kidney, RAGE/sRAGE balance shifted in the direction of RAGE in SHRob, matching the pro-fibrotic changes and functional deterioration observed. Renal RAGE/sRAGE was shifted to a more favourable ratio after RDN and correlated with renal norepinephrine concentrations as a measure of completeness of renal nerve ablation. These effects are partly independent of blood pressure but can be induced by direct ß-adrenergic activation in adult rat renal

fibroblasts and human embryonic kidney cells. The observations match with our previous results (**5**), where we demonstrated ß-adrenergic-induced in-vitro RAGE/sRAGE regulation in cardiac fibroblasts and peripheral blood mononuclear cells. We reproduced those results herein.

AGEs can cause renal tubular injury and promote tubular-interstitial fibrosis in chronic kidney disease (**17-19**). Interestingly, CML-levels were increased in SHRob as well as in lean SHR in our study. As both groups have hypertension, there might be a link between elevated blood pressure and CML formation, as suggested by several other groups (**26-27**). CML could act as indicator of long-term oxidative stress of the respective tissue (**28-29**) and has been shown to be associated with renal inflammation and diabetic nephropathy (**15**). It has been shown that CML accumulates in the proximal tubules of the kidneys during the development of hypertension (**30**), independent of the degree of nephropathy. In addition, deposits of AGEs not only promote fibrosis formation by e.g. RAGE-mediated inflammation and collagen production, but also inhibit collagenase mediated collagen degradation by cross-linking the collagen fibrils, making fibrosis more persistent (**31**).

HMGB1, a RAGE-ligand and Danger associated molecular pattern (DAMP) molecule, is released by activated immune cells as well as necrotic cells (**32**). It has been shown to induce tubulointerstitial inflammation in the kidney (**33**). Only a significant increase in SHRob was observed, suggesting a stronger inflammatory state in SHRob as compared with lean SHR. Again, HMGB1 levels were decreased after RDN. Recent data suggest that HMGB1 acts as an adipokine in metabolic syndrome (**34-35**) and plays a central role in the pathogenesis of insulin resistance (**36**), while RDN has been shown to improve glucose metabolism and insulin sensitivity in addition to reducing blood pressure in patients (**37**).

RDN is currently under investigation as a device-based therapy for uncontrolled hypertension (**38-40**). Recently published sham-controlled, clinical trials (**2-3; 41-42**) provided proof of principle for the blood pressure-lowering efficacy of RDN. Given the fact that various cardiovascular comorbidities are characterized by increased sympathetic activity, RDN may also represent a potential treatment in chronic kidney disease, and metabolic syndrome (**43-45**). The results presented herein provide the physiological basis for clinical studies in these conditions (**22-23**).

Limitations

The results are hypothesis-generating and need to be scrutinized in patients with metabolic syndrome and hypertension. However, there already are clinical studies reporting RDN-mediated beneficial effects on glucose metabolism and renal function (**22; 37; 46**).

The animal model for metabolic syndrome includes several individual risk factors and pathologies. As each one of them, including impaired glucose tolerance, hyperlipidemia or

hypertension could impact some of the observations made, we cannot assess the weight of the individual risk factors for renal damage. In order to assess the impact of hypertension only on the overall picture of the metabolic syndrome regarding RAGE/sRAGE regulation and organ remodelling, we included the SHR group in this study too. Further investigations on obesity and diabetes only and renal failure models with normal blood pressure are necessary to characterize the intricate network of pathologies and the influence of the sympathetic nervous system in each context.

Conclusion

Sympathoadrenergic activation in metabolic syndrome worsens RAGE/sRAGE balance leading to kidney end-organ damage. Disruption of renal sympathetic nerve fibres by RDN improves kidney function and interstitial remodelling with restored RAGE/sRAGE balance, reduction of RAGE ligands and anti-inflammatory and anti-fibrotic effects. These data may help to facilitate new therapeutic targets and strategies to prevent progressive loss in renal function in metabolic syndrome and provide potential mechanisms of RDN to protect the kidney.

Material and Methods

Animals

For this study, male 10-week-old rats of the species SHRs-ob (n = 12), SHR (n=6) and normotensive Sprague-Dawley rats (controls (Ctrs); n = 6) were acquired from Charles River (Sulzfeld, Germany). At the age of 34 weeks, RDN was performed in 6 SHRob, as described before (**6**). At this age, the animals had fully established a MetS with hypertension, nephropathy and hyperinsulinemia. SHRs-ob + RDN (n=6) were compared with 6 sham-operated SHRs-ob (SHR-ob) and sham-operated normotensive Ctrs and SHR, on which sham surgery with kidney exposure but without RDN was performed. Simultaneously to RDN, telemetric sensors were implanted for systolic and diastolic pressure and heart rate acquisition as described before (**6**). The animals were kept in standard cages for the duration of the study and were fed a standard Chow diet (standard diet No. 1320; Altromin, Lage, Germany) and tap water ad libitum. Rats were kept until the age of 48 weeks for the final experiments, after which the animals were sacrificed. The experiments were performed in accordance with the National Health Guideline for the Care and Use of Laboratory Animals as well as with the Animal Welfare Guidelines and the German Animal Welfare Act. The approval of the responsible regional committee was obtained.

Reagents

DMEM (Dulbecco´s Modified Eagle´s Medium) and M199 medium and FCS (fetal calf serum) were provided by Gibco/Invitrogen (Karlsruhe, Germany). Penicillin/streptomycin was purchased from Sigma-Aldrich (Deisenhofen, Germany), so were ß-adrenergic receptor selective antagonists CGP20712A (C231), ICI118.551 (I127) and isoproterenol (I6504). Rabbit polyclonal primary antibodies against the extracellular domain of human RAGE (ab37647), against HMGB1 (ab18256) and against CML (ab27684) were from Abcam (Cambridge, UK). HRP-conjugated secondary antibodies were from Sigma-Aldrich (Deisenhofen, Germany). Unless specified otherwise, all other substances used were from Sigma-Aldrich.

Blood, urine and tissue sampling

The rats were put in metabolic cages (Tecniplast, Buguggiate, Italy) for 24 hours and urine was collected for the determination of urine creatinine, albumin, and electrolyte concentrations. Measurements were performed by Hitachi 912 analyzer, Roche Diagnostics, Mannheim, Germany). Glomerular filtration rate was calculated as recently described (**6**). An oral glucose testing was performed (baseline measurement and after glucose loading with 2 g/kg body weight). Blood was obtained from the retro-orbital plexus (anesthesia with 3.5% isoflurane). Blood glucose, glycated hemoglobin (HbA1c), cholesterol, triglyceride and creatinine were measured using standard kits (Cobas Integra, Roche Diagnostics, Mannheim, Germany).

At the age of 45 weeks and after completion of invasive functional measurements, blood was extracted from the aorta and urine from the urinary bladder and stored at -80°C until further analysis. Kidneys were quickly excised, and tissue aliquots were snap-frozen in liquid nitrogen and stored at -80°C until further analysis. Norepinephrine measurement in kidney tissue was performed by high-pressure-liquid-chromatography (HPLC) (**6**).

Histological analysis

Parts of the left kidney were soaked in buffered 4% paraformaldehyde for 24 hours and subsequently embedded in paraffin for further histological analysis. Kidney sections of 3 µm thickness were prepared, deparaffined, rehydrated and stained with hematoxylin and eosin (HE) or Picro-Sirius red for further analysis. The Picro-Sirius-Red staining was used for visualization of interstitial and perivascular fibrosis. The percentage of interstitial collagen was given by the image analysis software (Nicon Instruments Software (NIS)-Elements (BR 3.2) as the ratio of the area positively stained with Picro-Sirius red to kidney total area, respectively. Furthermore, kidney sections were additionally stained with hematoxylin and eosin. After staining with hematoxylin and eosin, incidence and extent of glomerulosclerosis was assessed on a semi-quantitative basis by assessing glomerular damage: normal appearance (zero points); focal-segmental mesangial thickening in a few isolated glomeruli (one point); mesangial thickening in several glomeruli (2 points), diffuse/nodular mesangial thickening and synechia with Bowman's capsule in many but less than 50% of the glomeruli or diffuse glomerular sclerosis (3 points), if present in more than 50% of the glomeruli (4 points) or diffuse glomerulosclerosis and synechia with Bowman's capsule (5 points).

Immunofluorescence analysis for renal RAGE

RAGE immunostainings were performed on 3 µm paraffin sections of kidney tissue using heat-mediated antigen retrieval with 0.05% citraconic anhydride solution followed by overnight incubation at 4 °C and additional incubation for 2hours at 37°C with the 1:300 diluted primary antibody (Abcam; ab37647, rabbit polyclonal to RAGE) and incubation with the appropriate secondary antibody (TRITC-conjugated donkey anti-rabbit IgG (Jackson ImmunoResearch)) at 37 °C for 90 min (dilution 1:50). 1xPBS buffer with 0.1% Tween 20 was used for washing steps. Stained sections were counterstained with DAPI (Calbiochem, Germany), mounted with fluorescent mounting medium (Vectashield, Vector Laboratories, USA) and subjected to fluorescence microscopic analysis using a Nikon Eclipse epifluorescence microscope (Nikon, Germany) with appropriate filters.

Immunoblotting

Renal samples were homogenized with extraction buffer (10 mmol/l cacodylic acid (pH 5.0), 0.15 mol/l NaCl, 1 µmol/l ZnCl2, 20 mmol/l CaCl2, 1.5 mmol/l NaN3, and 0.01% (v/v) Triton X-100) and mixed 2:1 v/v with SDS-PAGE loading buffer. After denaturation (95°C, 5 min), the samples were separated on 10-15% SDS polyacrylamide electrophoresis gels (25 µg tissue/lane) and transferred to nitrocellulose membranes (Protran®, Schleicher & Schuell GmbH, Dassel, Germany) by semi-dry electrophoretic blotting (0.8 mA/cm^2). After blocking with 0.1% Western Blocking Reagent (Roche, Mannheim, Germany) membranes were incubated with primary antibodies for RAGE/sRAGE (ab37647, rabbit polyclonal to RAGE, 1:1000 dilution, Abcam, Cambridge, UK), HMGB1 (ab18256, rabbit polyclonal to HMGB1, 1:1000, Abcam) and CML (ab 27684, rabbit polyclonal to CML, 1:2000, Abcam) at 4°C for 12-16h. The goat anti-rabbit, goat-anti-mouse and rabbit anti-goat secondary antibodies were used at a dilution of 1:10000 and incubated for 60 min at RT. Proteins were visualized by enhanced chemiluminescence (Amersham Pharmacia Biotech, Freiburg, Germany). Membranes were stripped afterwards for GAPDH analysis as loading control: twice stripped for 15 minutes at 56°C with stripping buffer (62.5 nM Tris-HCl (pH 6.8), 2%SDS, 0.1 M 2-mercaptoethanol), then repeatedly washed with PBS (in mmol/L: NaCl 170, KCl 33, Na2HPO4 40 and KH2PO4 18, pH 7.2) for at least one hour and blocked again in PBS containing 5% nonfat dry milk for 120 min at room temperature. Autoradiographs were quantified by imaging densitometry and analysed by the “LabWorks 4.6“Software (LabWorks Image Acquisition and Analysis Software, UVP BioImaging Systems, Cambridge, UK). Data are presented as arbitrary units (AU) normalized to GAPDH and a control sample.

Isolation of primary rat renal fibroblasts and culture conditions

Sprague Dawley rats were sacrificed instantly under deep general anaesthesia with isoflurane, xylazine (Rompun®) and ketamine (Ketavet®). Both kidneys were removed and washed with phosphate buffered saline (PBS) containing antibiotics (1% penicillin/streptomycin), then cut into small pieces, which were repeatedly added to a digestion solution (0.07% trypsin, 0.05%

Type II collagenase) and kept under gentle shaking at 37 C° until the tissue completely dispersed. The digestion reaction was terminated by adding an equal volume of 10% FBS medium into the digestion supernatant. Cell suspension from digestion was centrifuged at 1000 rpm for 5 min, the supernatant was removed, and the pellet was re-suspended in 1-2 ml of medium with 10% FBS and seeded onto 10 cm plates. Renal fibroblasts attached to the plate. After ca. 3h incubation time, the supernatant containing mostly tubular cells and endothelial cells was discarded and the medium was replaced by M199 medium with 10% FBS and 1% penicillin/streptomycin. The renal fibroblasts remained attached to the plate and were incubated in a humidified 37°C, 5% CO_2 incubator (HEREUS). The culture medium was exchanged every 48 hours. The fibroblasts reached confluency after approximately 7 days. They were transferred to 6-well plates for further stimulation experiments.

Culture conditions for Human Embryonic Kidney cells (HEK)

HEK-293T cells were purchased from ATCC (ATCC CRL-3216) and were cultured on uncoated 6-well dishes in 2ml DMEM medium +10%FBS in humidified air (5% CO_2) at 37°C. After reaching 80% confluency, the cell culture medium was replaced by a low FBS hunger medium (0.1% FBS) for 24 hours. Every 24 hours the cells were stimulated with isoproterenol (0.1 µmol/l) in the presence or absence of ß-adrenergic receptor antagonists with differing selectivity (ß1-selective CGP 201712A, ß2-selective ICI 118.551) for a total stimulation period of 72 hours. The ß-blocker was added 30 min prior to isoproterenol. The cell culture supernatant of the stimulated HEK cells was asserved every 24 hours and analyzed for sRAGE release. The cells were harvested after 72 hours of stimulation and processed for cell fractionation: The cell pellets were resuspended in hypotonic buffer (in mmol/l: Tris 5, EDTA 1, MgCl2 5, pH 8.0, PMSF 1, Leupeptin 1; Aprotinin 5 ug/ml), incubated for 15 minutes at 4°C, then subjected to 100000 g ultracentrifugation (1h, 4 °C) to obtain a "cytosolic" (supernatant) and "membranous" fraction (pellet). The membrane fraction was resuspended in hypotonic buffer. Membrane fraction and cell culture supernatant were analyzed for RAGE/sRAGE content by Western blot analysis. The uniform total protein loading on the gel (50 µg/lane) was controlled by Ponceau Red staining (Dianova, Germany). The data are presented as arbitrary units (AU) in percent of a control, unless otherwise stated. The same stimulation and harvest protocol was used for primary rat renal fibroblasts (see above).

Statistical analysis

Results are presented as mean±SEM. Significance was estimated with two-way-ANOVA with Tukey´s post-hoc test for multiple comparisons. Normal distribution of data was tested by Kolmogorov-Smirnov and Liliefors test and Spearman´s or Pearsons´s correlations are shown as applicable. A p-value <0.05 was considered significant. GraphPadPrism (version 6.0; GraphPad Software, San Diego California, USA) was used for statistical analysis.

Disclosure statement

Funding

This work was supported by HOMFOR 2015/2016 to SRS, the German Heart Foundation (F/03/15 to SRS and DL) and the German Research Foundation (Deutsche Forschungsgemeinschaft, SFB/TRR 219 to SRS, DL, MH, AK, TS, JJ, FM and MB (M02/S02, S01, S03, M06, C04, C08)).

Conflict of interest

M.B. has received speaker honoraria for lectures and scientific advice from Abbott, AstraZeneca, Boehringer Ingelheim, Medtronic, Servier, Vifor and Novartis outside of the submitted work. F.M. is supported by Deutsche Gesellschaft für Kardiologie (DGK), has received scientific support and speaker honoraria from Bayer, Boehringer Ingelheim, Medtronic and ReCor Medical.

References

1. Wyatt CM, Textor SC. Emerging evidence on renal denervation for the treatment of hypertension. *Kidney Int.* 2018; 94: 644-646.

2. Böhm M, Kario K, Kandzari DE et al. Efficacy of catheter-based renal denervation in the absence of antihypertensive medications (SPYRAL HTN-OFF MED Pivotal): a multicentre, randomised, sham-controlled trial. *Lancet.* 2020; 395: 1444-1451.

3. Townsend RR, Mahfoud F, Kandzari DE et al. Catheter-based renal denervation in patients with uncontrolled hypertension in the absence of antihypertensive medications (SPYRAL HTN-OFF MED): a randomised, sham-controlled, proof-of-concept trial. *Lancet.* 2017; 390: 2160-2170.

4. Mahfoud F, Ukena C, Schmieder RE et al. Ambulatory blood pressure changes after renal sympathetic denervation in patients with resistant hypertension. *Circulation.* 2013; 128: 132-140.

5. Selejan SR, Linz D, Tatu AM et al. Sympathoadrenergic suppression improves heart function by upregulating the ratio of sRAGE/RAGE in hypertension with metabolic syndrome. *J Mol Cell Cardiol.* 2018; 122: 34-46.

6. Linz D, Hohl M, Schutze J et al. Progression of kidney injury and cardiac remodeling in obese spontaneously hypertensive rats: the role of renal sympathetic innervation. *Am J Hypertens.* 2014; 28: 256-265.

7. Schirmer SH, Sayed MM, Reil JC et al. Improvements in left ventricular hypertrophy and diastolic function following renal denervation: effects beyond blood pressure and heart rate reduction. *J Am Coll Cardiol.* 2014; 63: 1916-1923.

8. Mahfoud F, Urban D, Teller D et al. Effect of renal denervation on left ventricular mass and function in patients with resistant hypertension: data from a multi-centre cardiovascular magnetic resonance imaging trial. *Eur Heart J.* 2014; 35: 2224-2231b.

9. Schirmer SH, Sayed MMYA, Reil JC et al. Atrial remodeling following catheter-based renal denervation occurs in a blood pressure- and heart rate-independent manner. *JACC Cardiovasc Interv.* 2015; 8: 972-980.

10. Egaña-Gorroño L, López-Díez R, Yepuri G et al. Receptor for advanced glycation end-products (RAGE) and mechanisms and therapeutic opportunities in diabetes and cardiovascular disease: insights from human subjects and animal models. *Front Cardiovasc Med.* 2020 10; 7: 37.

11. Zhang L, Bukulin M, Kojro E et al. Receptor for advanced glycation end-products is subjected to protein ectodomain shedding by metalloproteinases. *J Biol Chem*. 2008; 283: 35507–35516.

12. Raucci A, Cugusi S, Antonelli A et al. A soluble form of the receptor for advanced glycation endproducts (RAGE) is produced by proteolytic cleavage of the membrane-bound form by the sheddase a disintegrin and metalloprotease 10 (ADAM10). *FASEB J.* 2008; 22: 3716-3727.

13. Sárkány Z, Ikonen TP, Ferreira-da-Silva F et al. Solution structure of the soluble receptor for advanced glycation end-products (sRAGE). *J Biol Chem*. 2011; 286: 37525-37534.

14. Linz D, Hohl M, Mahfoud F et al. Cardiac remodeling and myocardial dysfunction in obese spontaneously hypertensive rats. *J Transl Med.* 2012; 10: 187. doi: 10.1186/1479-5876-10-187.

15. Rabbani N, Thornalley PJ. Advanced glycation end-products in the pathogenesis of chronic kidney disease. *Kidney Int.* 2018; 93: 803-813.

16. Chen X, Ma J, Kwan T et al. Blockade of HMGB1 attenuates diabetic nephropathy in mice. *Sci Rep.* 2018; 8: 8319. doi: 10.1038/s41598-018-26637-5.

17. Tomino Y, Hagiwara S, Gohda T. AGE-RAGE interaction and oxidative stress in obesity-related renal dysfunction. *Kidney Int.* 2011; 80: 133-135.

18. Zhou LL, Cao W, Xie C et al. The receptor of advanced glycation end-products plays a central role in advanced oxidation protein products-induced podocyte apoptosis. *Kidney Int.* 2012; 82: 759-770.

19. Harcourt BE, Sourris KC, Coughlan MT et al. Targeted reduction of advanced glycation improves renal function in obesity. *Kidney Int.* 2011; 80: 190-198.

20. D'Agati V, Schmidt AM. RAGE and the pathogenesis of chronic kidney disease. *Nat Rev Nephrol.* 2010; 6: 352-360.

21. Santilli F, Blardi P, Scapellato C et al. Decreased plasma endogenous soluble RAGE, and enhanced adipokine secretion, oxidative stress and platelet/coagulative activation identify non-alcoholic fatty liver disease among patients with familial combined hyperlipidemia and/or metabolic syndrome. *Vascul Pharmacol.* 2015; 72: 16-24.

22. Mahfoud F, Cremers B, Janker J et al. Renal hemodynamics and renal function after catheter-based renal sympathetic denervation in patients with resistant hypertension. *Hypertension.* 2012; 60: 419-424.

23. Mahfoud F, Böhm M, Schmieder R et al. Effects of renal denervation on kidney function and long-term outcomes: 3-year follow-up from the Global SYMPLICITY Registry. *Eur Heart J.* 2019; 40: 3474-3482.

24. Peng Y, Kim JM, Park HS et al. AGE-RAGE signal generates a specific NF-κB RelA "barcode" that directs collagen I expression. *Sci Rep.* 2016; 6: 18822. doi: 10.1038/srep18822.

25. Eiros R, Romero-González G, Gavira JJ et al. Does chronic kidney disease facilitate malignant myocardial fibrosis in heart failure with preserved ejection fraction of hypertensive origin? *J Clin Med.* 2020; 9; 404. doi: 10.3390/jcm9020404.

26. Wang X, Desai K, Clausen JT et al. Increased methylglyoxal and advanced glycation end-products in kidney from spontaneously hypertensive rats. *Kidney Int.* 2004; 66: 2315-2321.

27. Rashid G, Benchetrit S, Fishman D et al. Effect of advanced glycation end-products on gene expression and synthesis of TNF-alpha and endothelial nitric oxide synthase by endothelial cells. *Kidney Int.* 2004; 66: 1099-1106.

28. Rivero A, Mora C, Muros M et al. Pathogenic perspectives for the role of inflammation in diabetic nephropathy. *Clin Sci (Lond)*. 2009; 116: 479-492.

29. Fu MX, Knecht KJ, Thorpe SR et al. Role of oxygen in cross-linking and chemical modification of collagen by glucose. *Diabetes.* 1992; 41 Suppl 2: 42-48.

30. Baumann M, Stehouwer C, Scheijen J et al. N epsilon-(carboxymethyl)lysine during the early development of hypertension*. Ann N Y Acad Sci*. 2008; 1126: 201-204.

31. Zhao J, Randive R, Stewart JA. Molecular mechanisms of AGE/RAGE-mediated fibrosis in the diabetic heart. *World J Diabetes*. 2014; 5: 860-867.

32. Lotze MT, Tracey KJ. High-mobility group box 1 protein (HMGB1): nuclear weapon in the immune arsenal. *Nat Rev Immunol.* 2005; 5: 331-342.

33. Ali BH, Al Za'abi M, Al Shukaili A et al. High-mobility group box-1 protein in adenine-induced chronic renal failure and the influence of gum arabic thereon. *Physiol Res.* 2015; 64: 147-151.

34. Shimizu T, Yamakuchi M, Biswas KK et al. HMGB1 is secreted by 3T3-L1 adipocytes through JNK signaling and the secretion is partially inhibited by adiponectin. *Obesity (Silver Spring)*. 2016; 24: 1913-1921.

35. Zhang J, Zhang L, Zhang S et al. HMGB1, an innate alarmin, plays a critical role in chronic inflammation of adipose tissue in obesity. *Mol Cell Endocrinol.* 2017; 454: 103-111.

36. Wang Y, Zhong J, Zhang X et al. The role of HMGB1 in the pathogenesis of type 2 diabetes. *J Diabetes Res.* 2016; 2016: 2543268. doi: 10.1155/2016/2543268.

37. Mahfoud F, Schlaich M, Kindermann I et al. Effect of renal sympathetic denervation on glucose metabolism in patients with resistant hypertension: a pilot study. *Circulation.* 2011; 123: 1940-1946.

38. Böhm M, Linz D, Urban D et al. Renal sympathetic denervation: applications in hypertension and beyond. *Nat Rev Cardiol*. 2013; 10: 465-476.

39. Böhm M, Mahfoud F, Ukena C et al. First report of the Global SYMPLICITY Registry on the effect of renal artery denervation in patients with uncontrolled hypertension. *Hypertension.* 2015; 65: 766-774.

40. Lauder L, Azizi M, Kirtane AJ et al. Device- based therapies for arterial hypertension. *Nat Rev Cardiol.* 2020. doi: 10.1038/s41569-020-0364-1.

41. Kandzari DE, Böhm M, Mahfoud F et al. Effect of renal denervation on blood pressure in the presence of antihypertensive drugs: 6-month efficacy and safety results from the SPYRAL HTN-ON MED proof-of-concept randomised trial. *Lancet.* 2018; 391: 2346-2355.

42. Azizi M, Schmieder RE, Mahfoud F et al. Endovascular ultrasound renal denervation to treat hypertension (RADIANCE-HTN SOLO): a multicentre, international, single-blind, randomised, sham-controlled trial. *Lancet.* 2018; 391: 2335-2345.

43. Veiga GL, Nishi EE, Estrela HF et al. Total renal denervation reduces sympathoexcitation to different target organs in a model of chronic kidney disease. *Auton Neurosci.* 2017; 204: 81-87.

44. Böhm M, Linz D, Ukena C et al. Renal denervation for the treatment of cardiovascular high risk-hypertension or beyond? *Circ Res.* 2014; 115: 400-409.

45. Mahfoud F, Azizi M, Ewen S et al. Proceedings from the 3rd European Clinical Consensus Conference for clinical trials in device-based hypertension therapies. *Eur Heart J.* 2020; 41: 1588-1599.

46. Hering D, Mahfoud F, Walton AS et al. Renal denervation in moderate to severe CKD. *J Am Soc Nephrol.* 2012; 23: 1250-1257.

Acknowledgements

The authors thank Laura Frisch for excellent technical assistance.

Figure legends

FIGURE 1

A) Representative histological pictures (picrosirius red staining) and

B) Quantification of renal fibrotic area (interstitial fibrillar collagen fractional area (%)) in normotensive controls (n=5), SHR (n=5), SHRob (n=6) and SHRobRDN (n=5).

C) Representative images (polarization microscopy) and

D) Quantification of collagen type I (red-yellow birefringence)/collagen type III (green birefringence) ratio in renal tissue of normotensive controls (n=5), SHR (n=5), SHRob (n=5) and SHRobRDN (n=5).

E) Representative histological pictures (hematoxyline eosin staining) and

F) Semi-quantitative assessment of glomerular damage (glomerular score) in renal tissue of normotensive controls (n=5), SHR (n=5), SHRob (n=5) and SHRobRDN (n=6).

**p<0.05 versus Control; § p<0.05 versus SHR; #p<0.05 versus SHRob.*

FIGURE 2

A) Representative fluorescence microscopy for RAGE (stained red by TRITC), kidney tissue autofluorescence (green) and nuclei (stained blue by DAPI) in kidneys of control rats (left

panel), SHR (first middle panel), SHRob (second middle panel) and SHRobRDN rats (right panel) (n=3 each group). Magnification 20x (upper panels) and 40x (lower panels). Scale bars 50 and 100 µm**.**

B) Representative Western blot (images from different parts of the same gel) and

C) Quantification of renal RAGE and

D) renal sRAGE in kidney homogenates from normotensive controls (n=5), SHR (n=5-6), SHRob (n=5) and SHRobRDN (n=5-6).

RAGE and sRAGE in arbitrary units (AU) normalized to GAPDH. **p<0.05 versus Control; § p<0.05 versus SHR; #p<0.05 versus SHRob.*

Correlation between E) renal RAGE and renal norepinephrine content, F) renal sRAGE and renal norepinephrine content in SHRob and SHRobRDN (n=10). Spearman correlation (p-value).

FIGURE 3

A) Representative Western blot (upper panel) of renal CML-modified proteins (images from different parts of the same gel) and quantification of CML (lower panel) in normotensive controls (n=5), SHR (n=5), SHRob (n=5) and SHRobRDN (n=5). CML in arbitrary units (AU) normalized to GAPDH.

The antibody recognizes carboxymethyllysine modified proteins species independently. The Western blot images show multiple bands belonging to different proteins.

B) Representative Western blot (upper panel) and quantification of renal HMGB1 (lower panel) in homogenates from normotensive controls (n=5), SHR (n=5), SHRob (n=5) and SHRobRDN (n=5). HMGB1 in arbitrary units (AU) normalized to GAPDH.

**p<0.05 versus Control; § p<0.05 versus SHR; #p<0.05 versus SHRob.*

FIGURE 4

A) Representative Western blot (upper panel) and quantification of membrane RAGE expression in HEK (lower panel) repeatedly stimulated with isoproterenol (ISO) 0.1 umol/l in the presence or absence of CGP (ß1-selective antagonist; 0.3 umol/l) or ICI (ß2-selective antagonist; 0.1 umol/l) for 72h every 24h. RAGE expression in arbitrary units (AU) with the control sample assigned a value of 1. n=4-8 per group.

B) Representative Western blot (upper panel; images from different parts of the same gel) and quantification of sRAGE secretion in supernatant of HEK (lower panel) repeatedly stimulated with isoproterenol (ISO) 0.1 umol/l in the presence or absence of CGP (ß1-

selective antagonist; 0.3 umol/l) or ICI (ß2-selective antagonist; 0.1 umol/l) for 72 h every 24h. sRAGE expression in arbitrary units (AU) with the control sample assigned a value of 1. n=4 per group.

**p<0.05 versus Control and ISO+CGP; #p<0.05 versus Control and ISO+ICI.*

FIGURE 5

A) Representative Western blot (upper panel) and quantification of membrane RAGE expression in renal fibroblasts (lower panel) repeatedly stimulated with isoproterenol (ISO) 0.1 umol/l (n=4) in the presence or absence of CGP (ß1-selective antagonist; 0.3 umol/l) or ICI (ß2-selective antagonist; 0.1 umol/l) for 72h every 24h. RAGE expression in arbitrary units (AU) with the control sample assigned a value of 1.

B) Representative Western blot (upper panel; images from different parts of the same gel) and quantification of sRAGE secretion in supernatant of renal fibroblasts (lower panel) repeatedly stimulated with isoproterenol (ISO) 0.1 umol/l (n=4) in the presence or absence of CGP (ß1-selective antagonist; 0.3 umol/l) or ICI (ß2-selective antagonist; 0.1 umol/l) for 72 h every 24h. sRAGE expression in arbitrary units (AU) with the control sample assigned a value of 1.

**p<0.05 versus Control; #p<0.05 versus Control and ISO+ICI.*

Figure 1

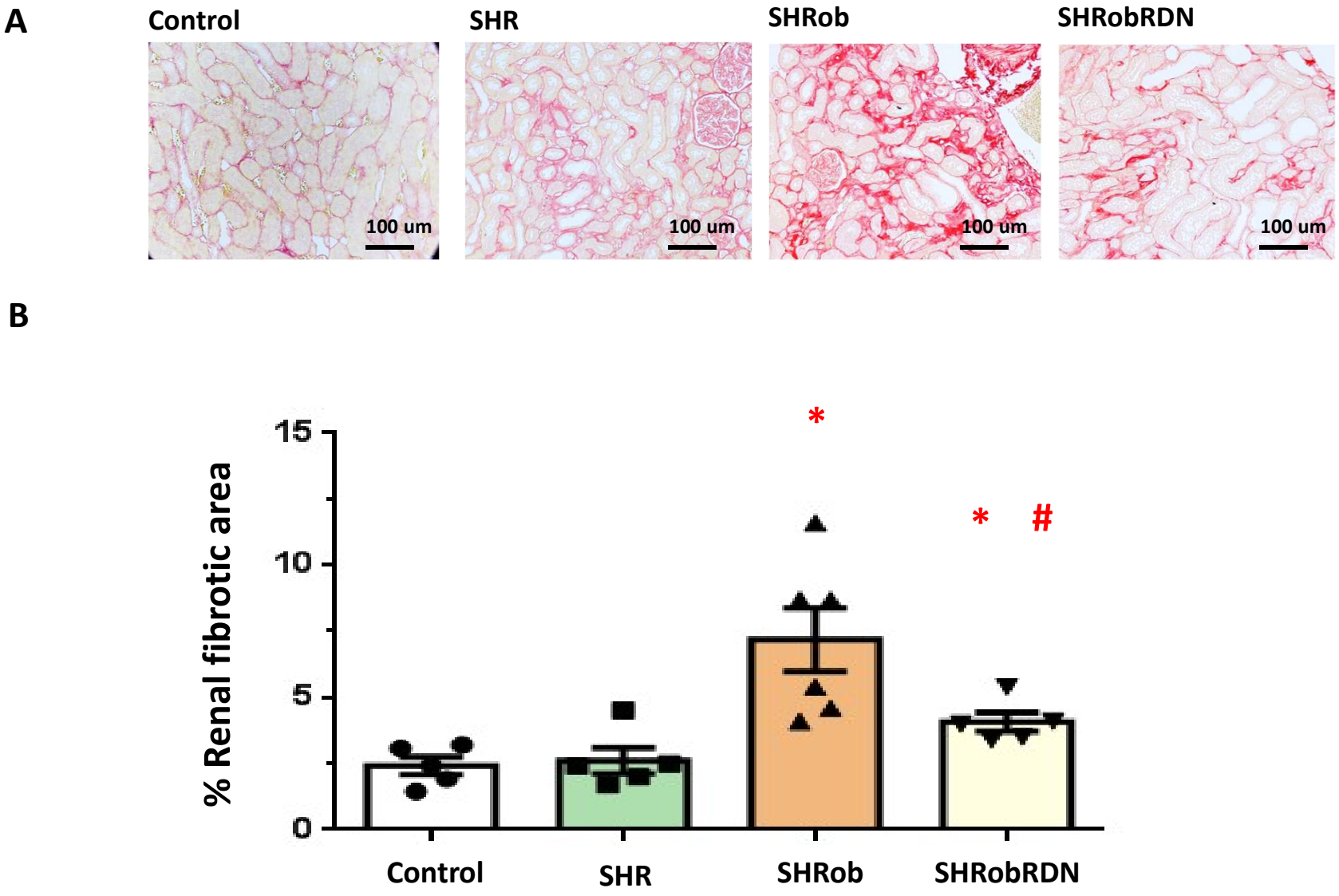
A
Control
SHR
SHRob
SHRobRDN
100 um
100 um
100 um
100 um
B
% Renal fibrotic area
15
10
5
0
*
* #
Control
SHR
SHRob
SHRobRDN

Figure 1

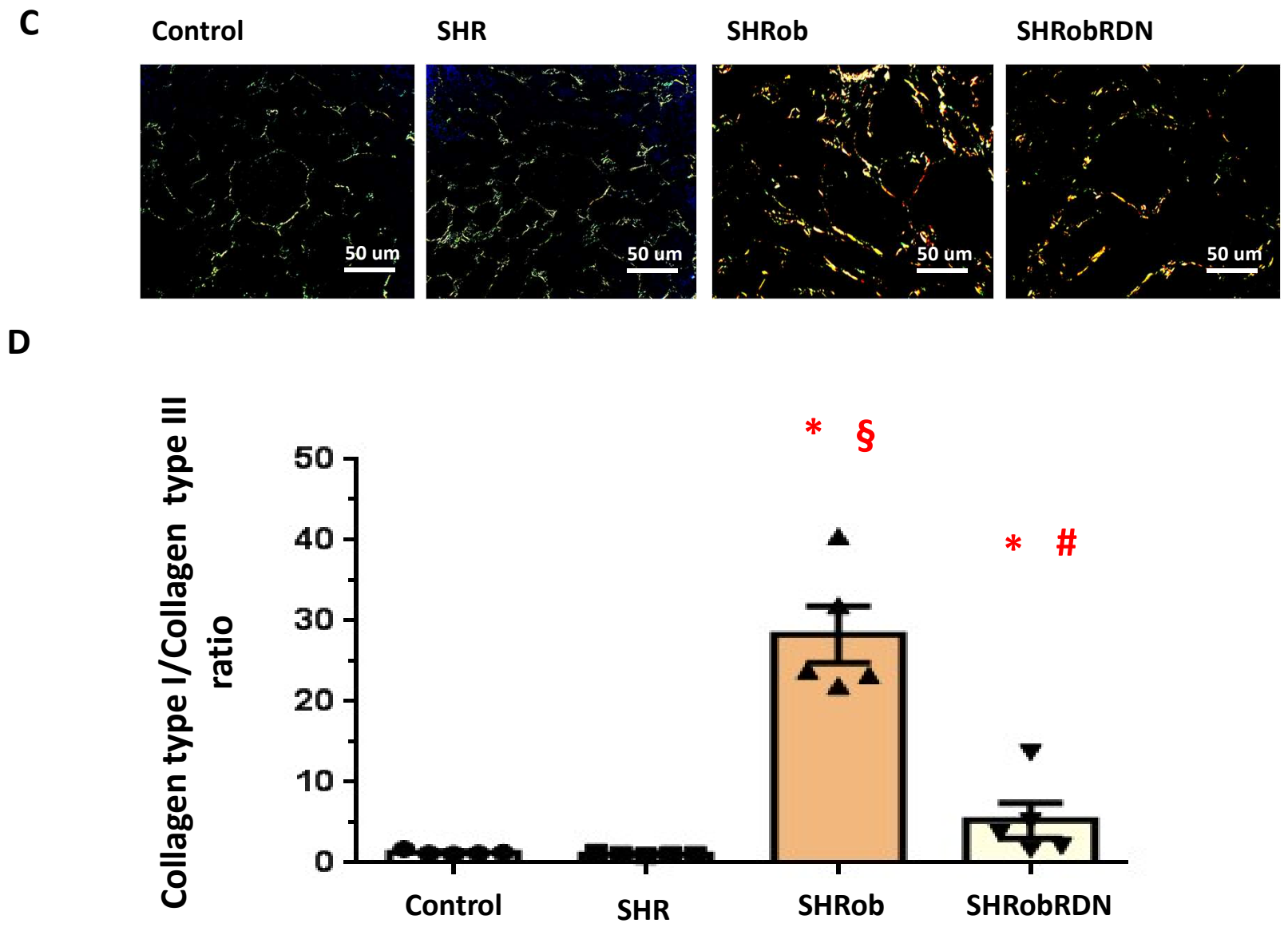
C
Control
SHR
SHRob
SHRobRDN
50 um
50 um
50 um
50 um
D
Collagen type I/Collagen type III ratio
50
40
30
20
10
0
* §
* #
Control
SHR
SHRob
SHRobRDN

Figure 1

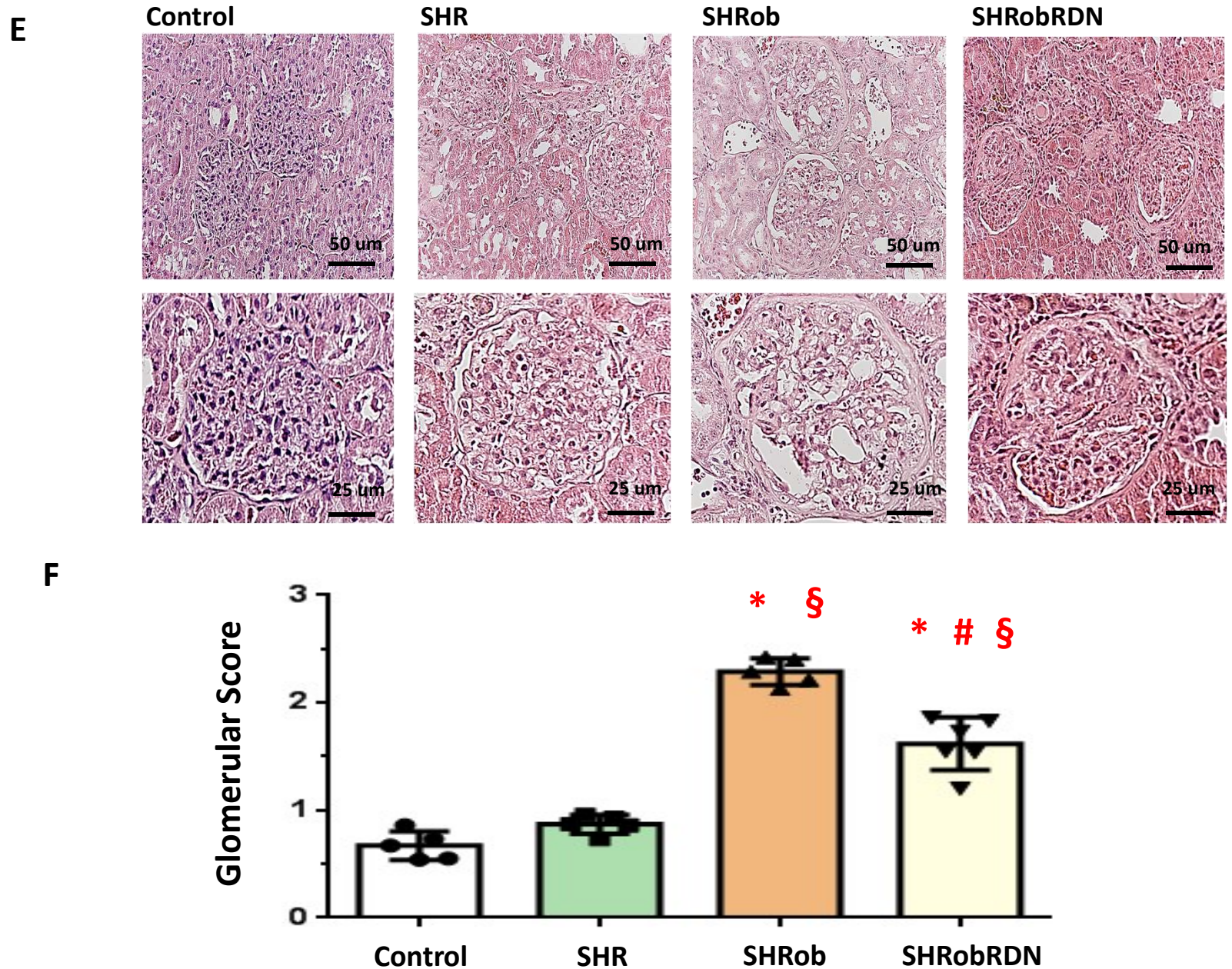
E
Control
SHR
SHRob
SHRobRDN
50 um
25 um
F
Glomerular Score
0
1
2
3
* §
* # §
Control
SHR
SHRob
SHRobRDN

Figure 2

A

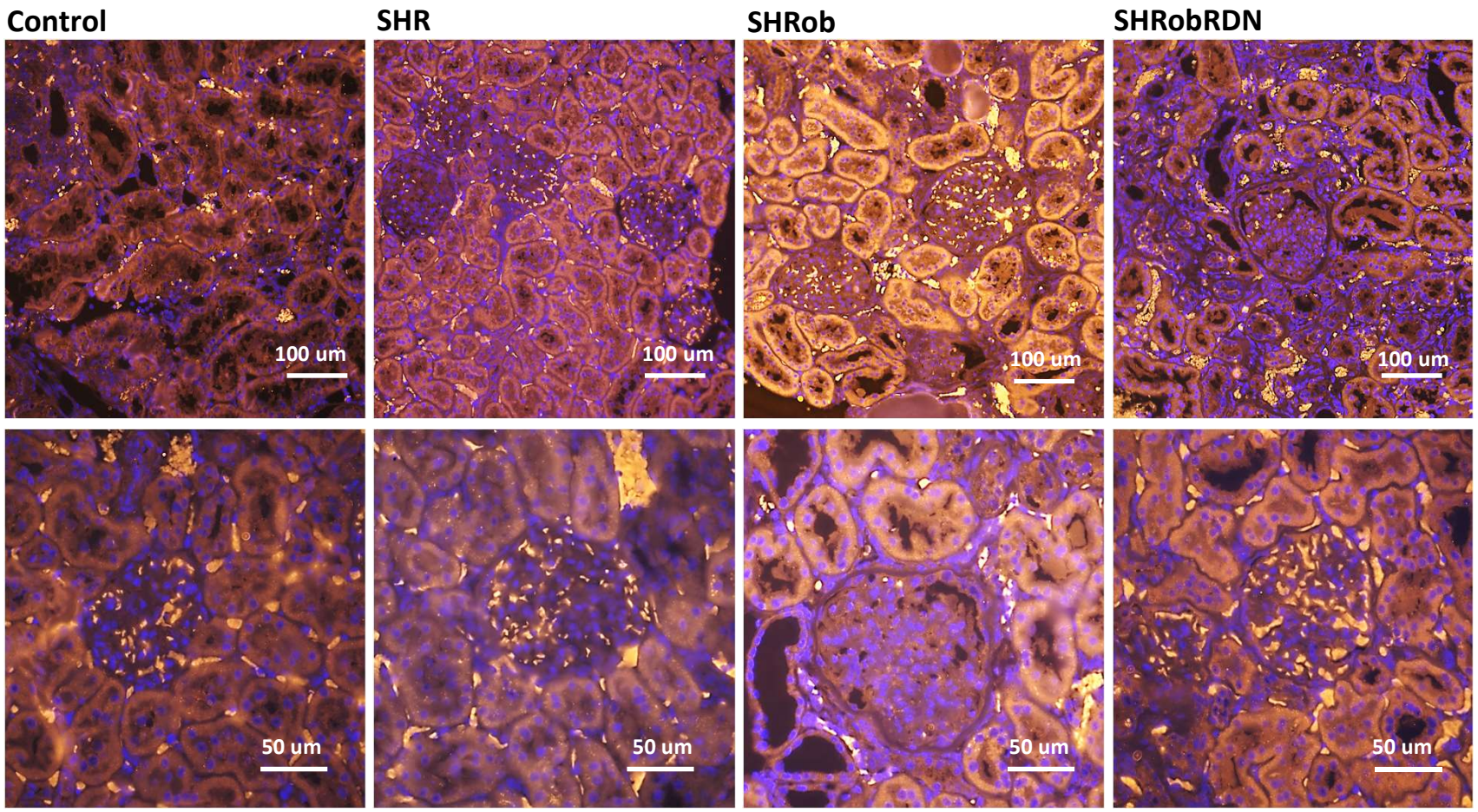
Control
SHR
SHRob
SHRobRDN
100 um
100 um
100 um
100 um
50 um
50 um
50 um
50 um

Figure 2

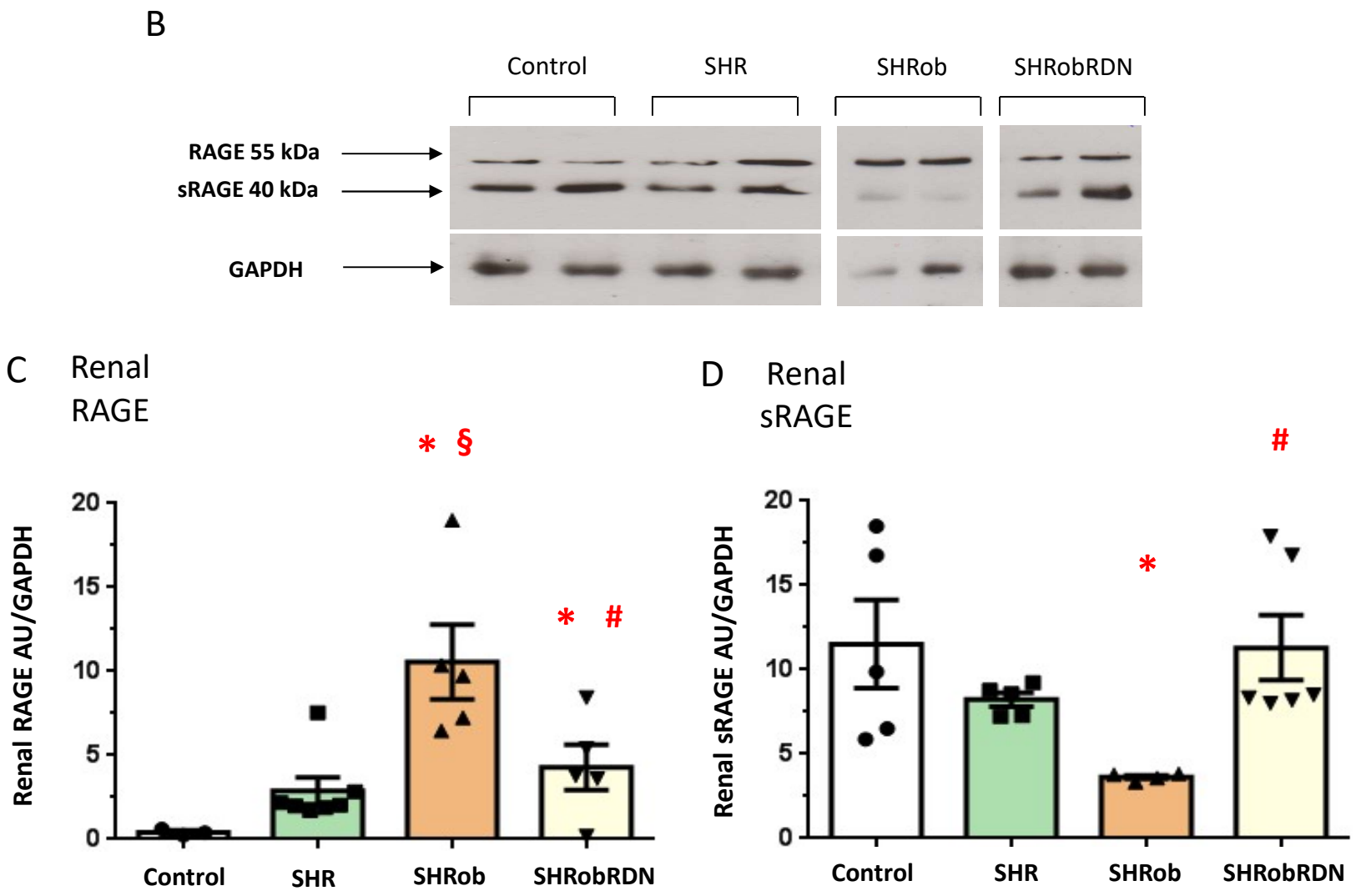
B
Control
SHR
SHRob
SHRobRDN
RAGE 55 kDa
sRAGE 40 kDa
GAPDH
C
Renal
RAGE
* §
* #
Renal RAGE AU/GAPDH
20
15
10
5
0
Control
SHR
SHRob
SHRobRDN
D
Renal
sRAGE
#
*
Renal sRAGE AU/GAPDH
20
15
10
5
0
Control
SHR
SHRob
SHRobRDN

Figure 2

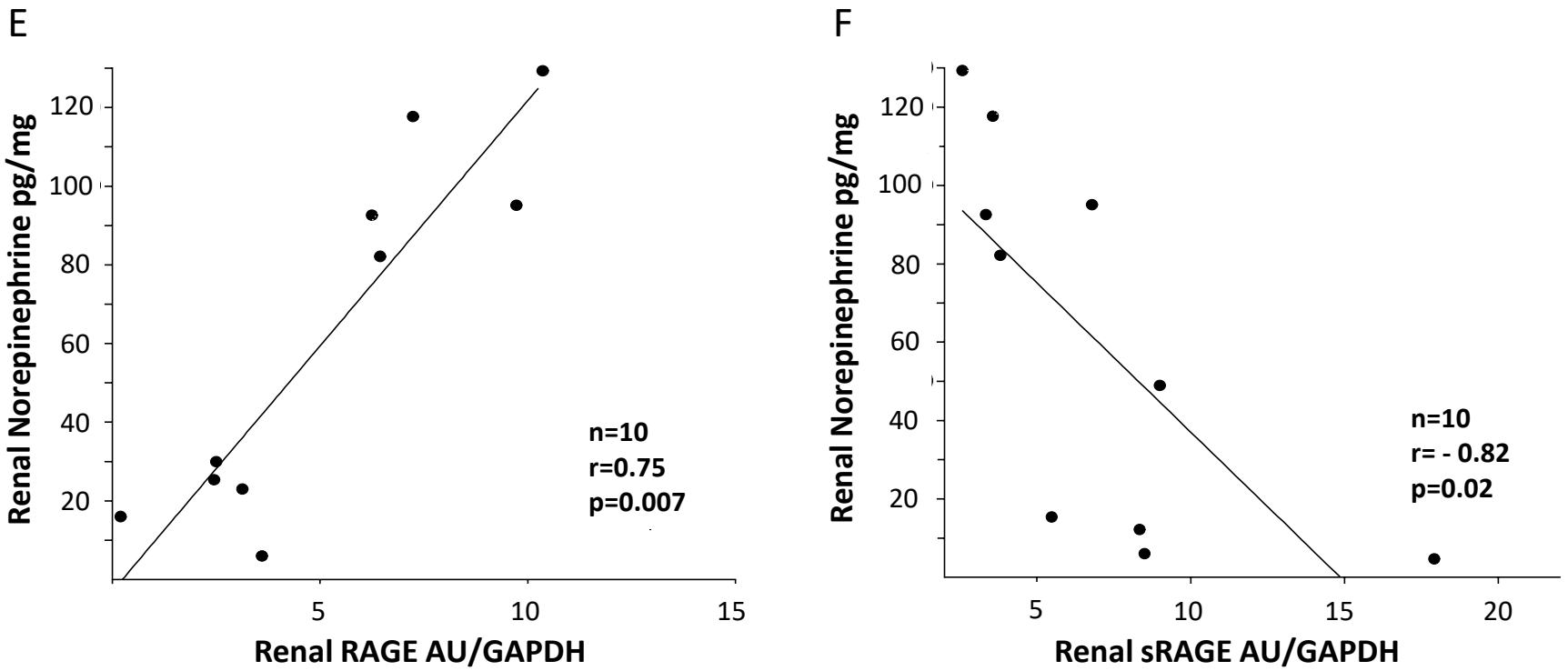
E
Renal Norepinephrine pg/mg
120
100
80
60
40
20
5
10
15
Renal RAGE AU/GAPDH
n=10
r=0.75
p=0.007
F
Renal Norepinephrine pg/mg
120
100
80
60
40
20
5
10
15
20
Renal sRAGE AU/GAPDH
n=10
r= - 0.82
p=0.02

Figure 3

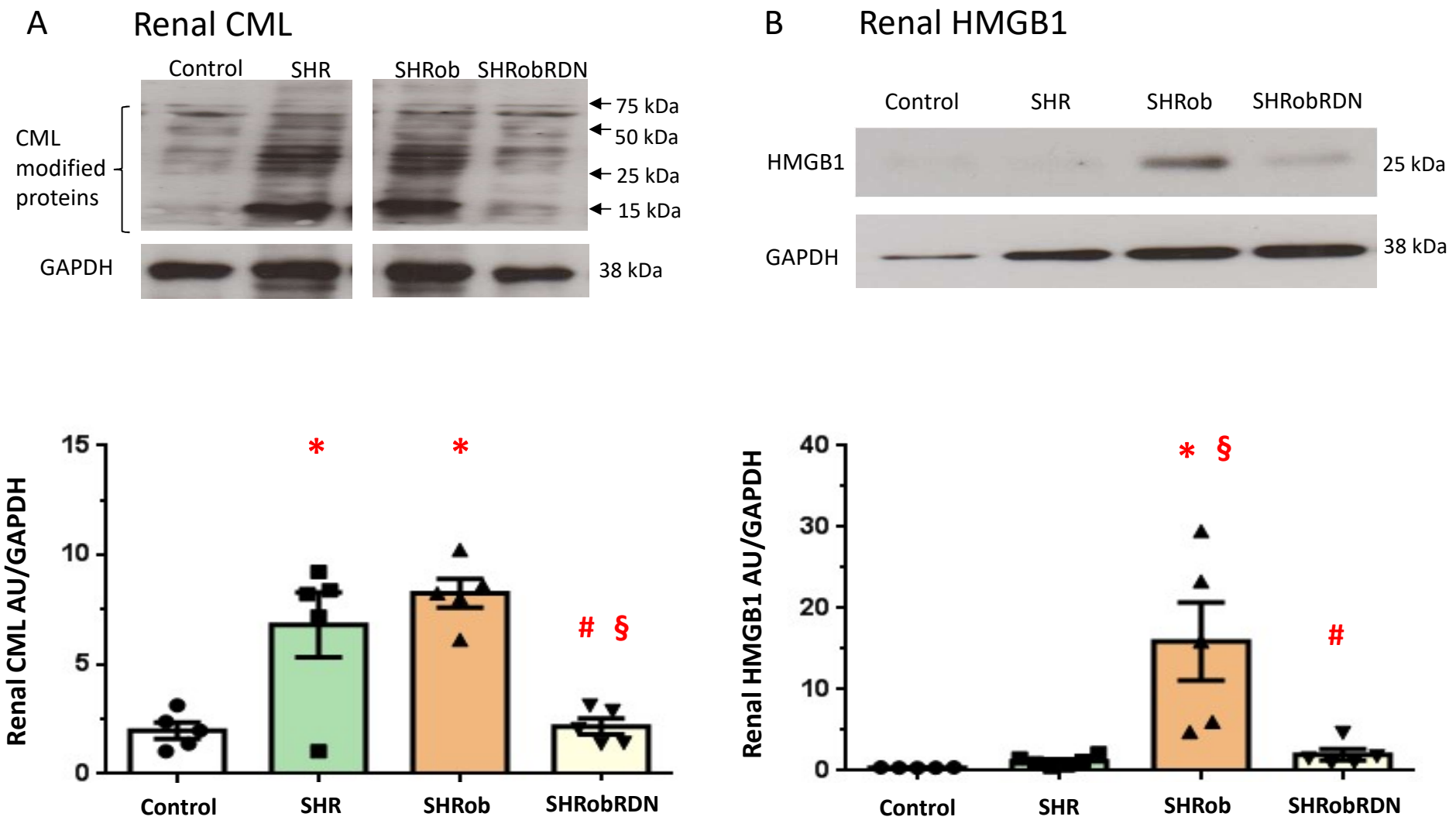
A
Renal CML
Control
SHR
SHRob
SHRobRDN
CML modified proteins
75 kDa
50 kDa
25 kDa
15 kDa
GAPDH
38 kDa
B
Renal HMGB1
Control
SHR
SHRob
SHRobRDN
HMGB1
25 kDa
GAPDH
38 kDa
Renal CML AU/GAPDH
15
10
5
0
*
*
§
Control
SHR
SHRob
SHRobRDN
Renal HMGB1 AU/GAPDH
40
30
20
10
0
* §
#
Control
SHR
SHRob
SHRobRDN

Figure 4 HEK (Human Embryonic Kidney cells)

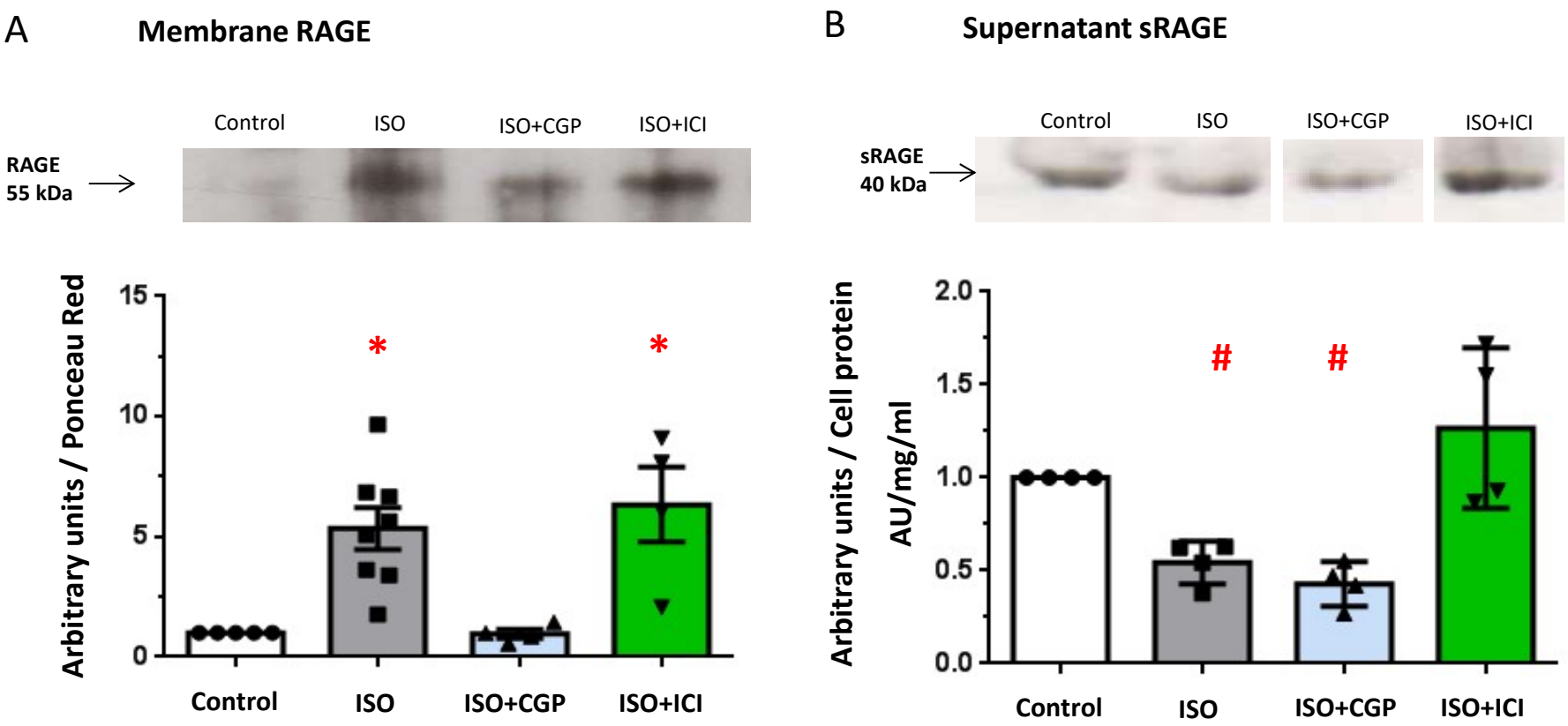

Figure 5 Renal fibroblasts

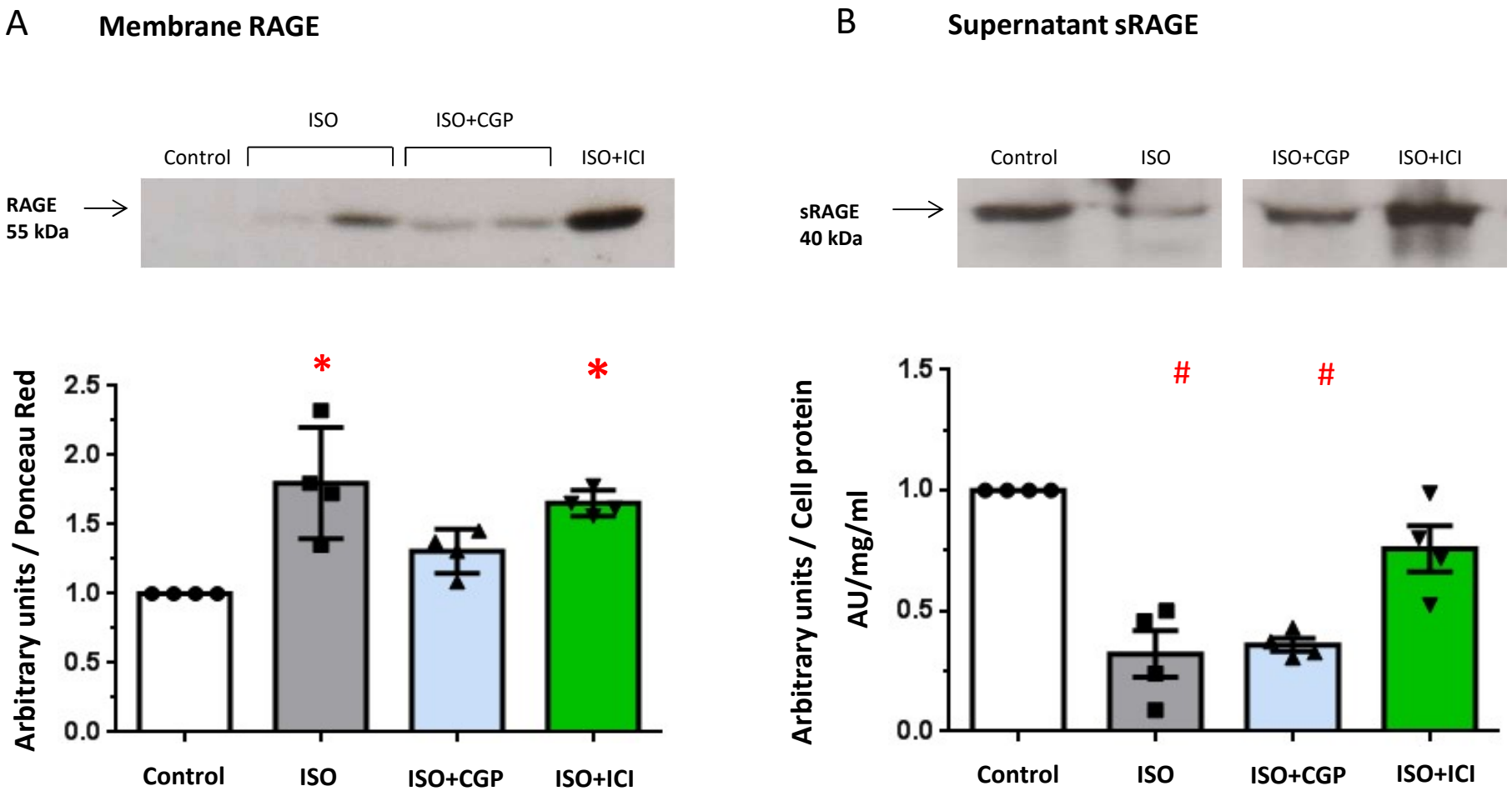

Table 1: Metabolic and renal parameters, RAGE/sRAGE, RAGE-ligands

	Controls N=5	**SHR N=5-6**	**SHRob N=5-6**	**SHRobRDN N=5-6**	**Ctrs vs. SHR**	**Ctrs vs. SHRob**	**Ctrs vs. SHRobRDN**	**SHR vs. SHRob**	**SHR vs. SHRobRDN**	**SHRob vs. SHRobRDN**
					p-values					
Creatinine umol/l	16.3±2.1	25±2.3	29±0.6	18.8±3.6	n.s	0.01	n.s	n.s	n.s	0.04
GFR l/kg/h	0.61±0.03	0.41±0.04	0.18±0.03	0.41±0.02	0.002	<0.001	0.002	<0.001	n.s.	<0.001
RR syst. mmHg	116±2.9	199±5.6	224±5	179±12.2	<0.001	<0.001	<0.001	0.04	n.s.	0.008
Glomerular Scoring	0.7±0.08	0.9±0.05	2.3±0.07	1.6±0.1	n.s	<0.001	<0.001	<0.001	<0.001	<0.001
Albuminuria (Albumine/ Creatinine ratio)	4.2±0.6	8±1.6	41.6±0.7	19.3±4.6	n.s	<0.001	0.005	<0.001	0.03	<0.001
Glomerular desmin %	3.9±0.8	24.2±5.7	28.3±1.5	10.5±2	0.003	0.001	n.s	n.s	0.02	0.008
Body weight	588±22	476±34	699±10	678±18	0.02	0.02	n.s	<0.001	<0.001	n.s
Glucose mmol/l	5±0.2	5.7±0.2	6.2±0.3	5.4±0.5	n.s	n.s	n.s	n.s	n.s	n.s
HbA1c%	3.5±0.07	3.5±0.05	3.8±0.2	3.7±0.07	n.s	n.s	n.s	n.s	n.s	n.s
Insulin pg/ml	929±111	1336±508	10626±2028	8592±225	n.s	<0.001	<0.001	<0.001	<0.001	n.s
Cholesterol mmol/l	3.8±0.1	3.9±0.2	9.6±0.1	9.4±0.4	n.s	<0.001	<0.001	<0.001	<0.001	n.s
Triglyceride mmol/l	1.73±0.1	1.8±0.2	5.7±0.2	5.5±0.3	n.s	<0.001	<0.001	<0.001	<0.001	n.s
Renal Norepinephrine pg/ml	85±3.6	94±4.1	103±5.5	8.2±2.2	n.s	0.04	<0.001	n.s	<0.001	<0.001
Renal RAGE AU/GAPDH	0.4±0.1	2.9±0.8	10.6±2.2	4.3±1.3	n.s	0.002	0.04	0.004	n.s	0.03
Renal sRAGE AU/GAPDH	11.9±3.3	8.2±0.4	3.6±0.1	11.3±1.9	n.s	0.04	n.s	n.s	n.s	0.04
Renal CML AU/GAPDH	1.98±0.5	6.8±1.5	8.3±0.9	2.2±0.4	0.02	0.003	n.s	n.s	0.01	0.003
Renal HMGB1 AU/GAPDH	1.1±0.2	1.78±0.5	15.9±6.2	1.98±0.7	n.s	0.01	n.s	0.004	n.s	0.01
Renal Interstitial Fibrosis %	2.4±0.3	2.9±0.3	7.2±1.2	4.1±0.4	n.s	0.008	0.04	0.01	n.s.	0.03

GFR: glomerular filtration rate; RR syst.: systolic blood pressure; BW: body weight; RAGE: Receptor for Advanced Glycation End products; sRAGE: soluble RAGE; CML: Carboxymethyllysine; HMGB1: High-Mobility-Group-Box-1; AU: arbitrary units; GAPDH: Glyceraldehyde 3-phosphate dehydrogenase